Air–Sea Feedback in the North Atlantic and Surface Boundary Conditions for Ocean Models

CLAUDE FRANKIGNOUL, ARNAUD CZAJA, AND BLANDINE L'HEVEDER

*Laboratoire d'Océanographie Dynamique et de Climatologie, Unité mixte de recherche CNRS-ORSTOM-UPMC,
Université Pierre et Marie Curie, Paris, France*

ABSTRACT

Extratropical sea surface temperature (SST) and surface turbulent heat flux monthly anomalies in the central and eastern part of the North Atlantic are considered for the period 1952–92 on a $5° \times 5°$ grid. In this region where the mean surface current is small, the SST anomalies are well simulated by a simple one-dimensional mixed layer model that is stochastically forced by the day-to-day changes in the local air–sea fluxes. A statistical signature of the stochastic model is that the cross correlation between surface heat flux and SST anomalies changes sign between negative and positive lags when the heat flux feedback is negative. This is observed at each grid point of the domain for the turbulent heat flux, which thus contributes both to generating the midlatitude SST anomalies and to damping them, once they are generated. Using properties of the lag covariance between SST and heat flux anomalies, the turbulent heat flux feedback is estimated from the observations. It averages to about 20 W m^{-2} K^{-1} in the investigated domain, increasing toward the northwest and the northeast and decreasing southward. It also varies seasonally, being generally largest in the fall and smaller and more uniform in summer. There is no indication that it can become significantly positive. A negative turbulent heat flux feedback is also suggested by the lag relation between the dominant modes of SST and turbulent heat flux variability over the whole North Atlantic, and it is found that the spatial patterns of the associated SST and turbulent heat flux anomalies are remarkably similar whether the atmosphere leads or lags, with only a change of heat flux sign between lead and lag situations.

This analysis provides some observational support for the use on short timescales of a restoring condition for SST in ocean-only simulations, but the coupling coefficient should be weaker than usually assumed and a function of latitude and season. The associated SST–evaporation feedback has little effect on interannual surface salinity changes. It should be significant on longer timescales, but then the restoring temperature should be allowed to vary and nonlocal influences should be considered.

1. Introduction

Since the atmosphere has a small heat capacity and a fast adjustment time, it is sometimes speculated that studies of long-term climate changes do not require the use of a fully prognostic atmospheric model, but rather can be based on simple representations of the atmosphere. The crudest one, which reduces the role of the atmosphere to prescribing a surface boundary condition, is often used in ocean-only modeling studies in the form of mixed boundary conditions combining a restoring boundary condition on surface temperature and an imposed freshwater flux. Although the thermohaline circulation is stable when restoring conditions are imposed for both surface temperature and salinity, it may have multiple equilibria and produce oscillations ranging from tens to thousands of years when mixed boundary

conditions are used (e.g., Stommel 1961; Bryan 1986; Marotzke and Willebrand 1991; Weaver and Sarachick 1991). However, the nature of the oscillations, sometimes even their existence, is dependent on the details of the mixed boundary conditions. In particular, the thermohaline circulation becomes generally more stable as the sea surface temperature (SST) restoring term becomes weaker (e.g., Zhang et al. 1993; Yin and Sarachik 1995; Chen and Ghil 1995). The latter can be written as

$$Q_r = \alpha(T^* - T), \qquad (1)$$

where Q_r has the form of a heat flux into the ocean, α is the coupling coefficient or feedback factor, T the SST, and T^* the prescribed restoring temperature often taken as an apparent (Haney 1971) or the observed mean air temperature. The restoring timescale is $\rho C_p H/\alpha$, where ρ is the density, C_p the specific heat of sea water, and H the upper-layer thickness. Most modeling studies have used a reference damping time of about one month, which corresponds to a negative heat flux feedback factor α of 80 W m^{-2} K^{-1} for H approximately equal to

Corresponding author address: Dr. Claude Frankignoul, LODYC Case 100, Universite Pierre et Marie Curie, 4 place Jussieu, 75252 Paris CEDEX, France.
E-mail: cf@lodyc.jussieu.fr

50 m. This is twice as much as the values derived from climatology by Haney (1971) or Han (1984) by assuming no atmospheric adjustment to SST changes. However, as the atmosphere adjusts to the underlying SST, the heat flux sensitivity $\partial Q/\partial T$ should be even weaker. Bretherton (1982) and Frankignoul (1985) have shown that SST anomalies should be more weakly damped at large scales, and the latter has suggested that, because of a phase shift between SST and heat flux response, the feedback may be positive on the eastern side of the SST anomaly and the atmosphere may act as an eastward propagator for the SST anomalies. Scale dependence in the restoring boundary condition for ocean models has been introduced by Rahmstorf and Willebrand (1995), who considered a simple energy balance model of the atmosphere with a diffusive heat transport and obtained values of α decreasing from 50 W m^{-2} K^{-1} at a 400-km scale to a few W m^{-2} K^{-1} at the largest scales. The more refined simplified model of the lower atmosphere designed by Kleeman and Power (1995) also predicts a decrease of the damping with increasing scale, and in Power et al. (1995) the heat flux response to a North Atlantic SST anomaly was generally restorative with α around 20 W m^{-2} K^{-1}, except for a positive feedback over its eastern flank.

As discussed in Frankignoul (1985), the heat flux feedback is dominated by the turbulent heat fluxes (latent and sensible heat flux), and it can be estimated from the response of atmospheric general circulation models (AGCMs) to prescribed SST anomalies. However, the relationship between the SST and heat flux anomaly fields may be rather complex and seems model dependent and, in some cases, a function of the location and polarity the SST anomaly. Frankignoul (1985) considered the January response of three AGCMs to a (mostly) negative SST anomaly in the North Pacific and found that the surface heat flux would cause a negative feedback of 16 and 20 W m^{-2} K^{-1} in two cases, but no feedback in a third one. Using different AGCMs, Kushnir and Lau (1992) found a weak negative feedback for a (mostly) positive North Pacific SST anomaly but no simple response for a (mostly) negative one, while Latif and Barnett (1994) found a very strong positive feedback to a mostly positive SST anomaly. Response studies with prescribed SST anomalies in the North Atlantic have also provided differing results. In Palmer and Sun (1985) the surface evaporation response was in phase with the SST anomaly, corresponding to a negative heat flux feedback. Similarly, in Kushnir and Held (1996) the surface heating was almost in phase with the SST anomaly, yielding a negative feedback of about 20 W m^{-2} K^{-1} in January conditions, and a slightly weaker one in October conditions, with only a small dependence on the SST polarity. In Power et al. (1995), the yearly averaged GCM response to a negative SST anomaly was found to be generally restorative with $\alpha \approx$ 10–20 W m^{-2} K^{-1}, although the feedback was positive on the eastern flank of the anomaly. In Peng et al. (1995), there

was only a significant atmospheric response for a positive SST anomaly, and it strongly depended on the basic flow. In November conditions, the turbulent heat flux feedback was strongly positive (we estimate it from their Fig. 21 to be about -10 W m^{-2} K^{-1} for the sensible heating alone), while in January conditions it was reported to be twice as strong, but negative.

In view of this disparity, it would be of interest to determine the heat flux feedback directly from the observations. As reviewed by Frankignoul (1985, 1995), the extratropical SST anomalies can be well simulated by a mixed-layer model, which is stochastically forced by the day-to-day changes in the local air–sea fluxes. The surface heat exchanges strongly contribute to generating the SST anomalies, but also to damping them once they are generated. However, this damping has not been hitherto quantified in the observations where cause and effect are difficult to distinguish. In the present paper, we show that a direct estimate of the heat flux feedback can be derived from the observed lag covariance between SST and heat flux anomalies if the mean surface current is small, and we estimate the turbulent heat flux feedback from anomaly data in the quiet part of the North Atlantic.

In section 2, we introduce the stochastic SST anomaly model and discuss the nature of the turbulent heat flux feedback. In section 3, we investigate its statistical signature and show how the observations can be used for its estimation. In section 4, the analysis is applied to 41 years of monthly midlatitude observations in the central and eastern North Atlantic. The dominant spatial patterns of the two-way air–sea interactions are also discussed, and their extension to the western North Atlantic is documented. In section 5, the seasonal dependence of the feedback factor is investigated, and in section 6 the boundary conditions for ocean-only simulations are briefly discussed.

2. The stochastic SST anomaly model

In a simple slab mixed-layer model where the temperature T and the horizontal current $\mathbf{u}$ are constant within a mixed layer of depth h, the vertically integrated temperature equation can be written

$$h(\partial_t T + \mathbf{u} \cdot \nabla T) + \Gamma(w_e)w_e(T - T^-)$$

$$= \frac{Q - Q^-}{\rho C_p} + \kappa h \nabla^2 T, \tag{2}$$

where Γ is the heaviside function; w_e the entrainment velocity; κ the horizontal mixing coefficient; Q the surface heat flux into the ocean (positive downward) given by the sum of latent heat flux Q_L, sensible heat flux Q_S, shortwave radiation Q_{SW}, and longwave radiation Q_{LW}; Q^- is the heat flux at the mixed-layer base, and the minus index indicates values just below the mixed layer. If the mixed layer is deepening, there is entrainment of colder water, whereas if it is becoming shallow, there

is detrainment and fluid is left behind without changing the SST. On short timescales, the mixed layer depth h is primarily determined by the turbulent kinetic energy budget, which is dominated by the energy transfer from the wind, surface heat exchanges, and turbulent dissipation.

Each field can be decomposed into a seasonally varying mean (denoted by an overbar) and an anomaly (denoted by a prime). To a good approximation, the equation for large-scale SST anomalies on the monthly to yearly timescales can be written (Frankignoul 1985) as

$$\frac{dT'}{dt} \approx \frac{\mathbf{u}'_{\mathrm{E}} \cdot \boldsymbol{\nabla}\overline{T}}{\overline{h}} - \frac{h'}{\overline{h}}\partial_t\overline{T} - \frac{[\Gamma(w_e)w_e(T - T^-)]'}{\overline{h}}$$
$$+ \frac{Q' - Q^{-'}}{\rho C_p \overline{h}} + \kappa\nabla^2 T', \tag{3}$$

where $d/dt = \partial_t + \overline{\mathbf{u}} \cdot \boldsymbol{\nabla}$ is the time derivative following the mean motion and $\mathbf{u}_{\mathrm{E}}$ is the Ekman transport. We have omitted the stirring by the mesoscale eddies, which primarily contributes a small-scale noise, and the modulation by variable large-scale geostrophic currents, which contributes to very low frequency SST changes.

In extratropical latitudes, the atmospheric forcing is dominated by the day-to-day changes in the weather and has a primarily white frequency spectrum at low frequencies. Over most of the extratropical oceans, the main SST anomaly forcing is by surface heat exchanges and vertical entrainment, although anomalous Ekman advection also plays a role in frontal zones. The turbulent heat fluxes dominate the heating anomalies in fall and winter, while Q'_{SW} is of comparable magnitude in spring and summer. Heat flux forcing dominates wind stirring from late fall to early summer, whereas the reverse is true from midsummer to midfall (Frankignoul 1985; Cayan 1992a; Alexander and Deser 1995). Because of its small mechanical inertia, the oceanic mixed layer responds rapidly to this forcing and h' also has a short characteristic timescale and a white spectrum at low frequencies, as shown by observed and simulated data (Cane and C. Frankignoul 1997, unpublished manuscript; Alexander and Penland 1996). The forcing part of the terms in (3) can thus be represented at low frequencies by a white noise process, which will be hereafter denoted by F'. This white noise forcing creates growing SST anomalies whose amplitude is limited by dissipation and feedback processes (Frankignoul and Hasselmann 1977).

As discussed by Frankignoul (1985), the main oceanic feedback involves entrainment and mixing, although the effective diffusion by surface current fluctuations may also play a role (Molchanov et al. 1987). The atmosphere primarily feeds back onto the SST anomalies, once have been generated, via the turbulent heat fluxes; however, in the AGCM experiments of Palmer and Sun (1985), the atmospheric ajustment was hypothesized to induce a positive feedback via Ekman advection. A small feedback may also be associated with SST anomaly-induced changes in the radiation fluxes.

For small SST anomalies, dissipation and feedback can be represented to a good approximation by linearizing the (in part hidden) T' dependence of the right-hand side of (3), that is, by only keeping the first two terms of its Taylor expansion in T'.

In regions of small mean current, the SST anomaly equation then takes the approximate form

$$\partial_t T' = F' - \lambda T', \tag{4}$$

where F' represents the stochastic forcing component of the right-hand side of (3), that is, the part that is not significantly affected by the SST anomalies but controlled by the dynamics of the free atmosphere,[1] and λ is a scale-dependent feedback factor, which includes the atmospheric boundary layer adjustment to the SST anomalies. The feedback factor is positive when the feedback is negative. If the seasonal modulation is neglected and the forcing white, (4) represents a first-order autoregressive or Markov process. The frequency spectrum of the SST anomalies is red and their autocovariance function given by

$$R_{TT}(\tau) \approx \frac{\pi}{\lambda}F_{FF}(0)e^{-\lambda|\tau|}, \tag{5}$$

for $\tau \gg \tau_F$, where τ_F denotes the atmospheric correlation timescale. Here $F_{FF}(0)$ is the white noise level of the forcing, $R_{XY}(\tau) = \langle X'(t + \tau)Y'(t)\rangle$ is the covariance between X' and Y' at lag τ, and the angle brackets denote ensemble mean. From (4), one finds

$$\partial_\tau R_{TF} = R_{FF} - \lambda R_{TF}, \tag{6}$$

so the covariance between T' and F' can be calculated, providing a statistical signature of the air–sea interactions (section 3). The stochastic forcing model can easily include the advection by the mean flow and can provide a valid representation of the SST anomalies over most of the midlatitudes, with an SST anomaly decay time λ^{-1} on the order of 3 months (Reynolds 1978; Frankignoul and Reynolds 1983; Herterich and Hasselmann 1987).

The atmospheric feedback is dominated by the fluxes of sensible and latent heat, which can be estimated from the bulk formulas

$$Q_{\mathrm{S}} = \rho^a C_p^a C_S u^a (T^a - T) \quad \text{and} \tag{7}$$

$$Q_{\mathrm{L}} = \rho^a L C_L u^a (q^a - q_s), \tag{8}$$

where the superscript a indicates atmospheric variables at 10 m, L is the latent heat of evaporation, u the wind speed, q the specific humidity, q_s the saturation specific humidity at the sea surface, C_p^a the air specific heat at constant pressure, and C_S and C_L bulk exchange coefficients. Assuming in a first approximation that u^a is not affected by T' leads to the sensible heating feedback, which is given in the same units as in (1) by

---

[1] This neglects the possible, but small, modulation of the statistical properties of F' by T'.

$$\rho C_p \overline{h} \lambda_{Q_S} \approx \rho^a C_p^a C_S u^a \frac{\partial}{\partial T'}(T' - \langle T^{a\prime} \rangle), \qquad (9)$$

where the angle brackets denote ensemble mean for given T' (or an average over many realizations of the atmospheric fields) and u^a is an appropriate wind speed. Assuming that the relative humidity remains constant and using the Clausius–Clapeyron equation to relate the saturation vapor pressure to the temperature yields similarly the feedback due to evaporation, given in SI units by

$$\rho C_p \overline{h} \lambda_{Q_L} \approx \rho^a L C_L u^a \frac{1.2 \times 10^{10}}{\overline{T}^2} e^{5388/\overline{T}} \frac{\partial}{\partial T'}$$

$$\times [(T' - R_h \langle T^{a\prime} \rangle)]. \qquad (10)$$

The degree of adjustment of the atmospheric boundary layer to an SST anomaly determines the feedback strength. If the air temperature was not affected by the SST anomaly, one would have $(\partial/\partial T')\langle T^{a\prime} \rangle = 0$ and there would be a strong negative feedback. Indeed, for $\overline{T} = 290$ K, $u^a = 8$ m s^{-1}, $R_h = 0.8$, $C_S = C_L = 1.3 \times 10^{-3}$, one finds

$$\rho C_p \overline{h} \lambda_{Q_S} \approx 12 \text{ W m}^{-2} \text{ K}^{-1} \quad \text{and} \qquad (11)$$

$$\rho C_p \overline{h} \lambda_{Q_L} \approx 38 \text{ W m}^{-2} \text{ K}^{-1}, \qquad (12)$$

which together amount to 50 W m^{-2} K^{-1}. Such a strong heat flux feedback is not realistic since it alone would imply a 2-month SST anomaly decay time for $\overline{h} = 70$ m. However, the air temperature in the atmospheric boundary layer adjusts somewhat to an SST change and the feedback critically depends on the dynamic response of the atmosphere to the SST anomaly. Barsugli and Battisti (1998) have recently extended the model (4) to include the latter, albeit in a simple, one-dimensional way. They assumed that the heat flux was proportional to the air–sea temperature difference and the surface air temperature linearly related to a free atmosphere temperature. The latter was determined by a simplified energy equation where the atmospheric dynamics was represented by a stochastic forcing term, so an explicit modulation of the heat flux forcing by the SST anomalies was allowed.

However, as discussed by Kushnir and Held (1996), there is no fully accepted theoretical framework to fully understand the dynamic response of the atmosphere to extratropical SST anomalies. While the linear atmospheric response to extratropical heat sources in a zonally symmetric flow is weak and baroclinic in the vicinity of the heat source, that of models linearized about zonally asymmetric basic states can be resonant and equivalent barotropic. AGCM experiments show much disparity. In some experiments the response is baroclinic (e.g., Kushnir and Held 1996), but in most cases the SST anomaly primarily displaces the storm track and alters the upper-tropospheric eddy vorticity flux and the equivalent barotropic structure of the atmosphere (e.g.,

Palmer and Sun 1985; Kushnir and Lau 1992; Peng et al. 1995). The relations among T', $\langle T^{a\prime} \rangle$, and the free atmosphere are thus poorly understood and seem model dependent. Hence, a direct estimation of the heat flux feedback from observations is of interest.

3. Statistical signature of the heat flux feedback

To single out the contribution of the surface heat flux to SST anomaly changes, we write (4) as

$$\partial_t T' = H' + m' - \lambda_0 T', \qquad (13)$$

where

$$H' = \frac{Q'}{\rho C_p \overline{h}} \qquad (14)$$

is the heat flux term; m' represents the other stochastic forcing terms, which are primarily associated with wind stress changes; and λ_0 represents all the contributions to the feedback that are not included in Q'. In section 4, λ_a will be estimated from turbulent heat flux data only and thus the contribution from the radiative fluxes will then be included in λ_0.

Since surface heat exchanges contribute both to SST anomaly generation and feedback, H' is decomposed into

$$H' = q' - \lambda_a T', \qquad (15)$$

where q' represents the stochastic forcing component of the heat flux anomalies (that part of the heat flux that is controlled by the large-scale atmospheric dynamics and is not influenced by the SST anomaly) and λ_a the heat flux feedback factor. One has $\lambda = \lambda_a + \lambda_0$ and $F' = q' + m'$.

From (13) and (15), the covariance between T' and q' obeys

$$\partial_\tau R_{Tq} = R_{qq} + R_{mq} - \lambda R_{Tq}. \qquad (16)$$

For algebraic simplicity, we assume that q' and m' can be represented as first-order Markov processes with the same atmospheric decay time ν^{-1}, a variance ratio of n^2, and a correlation, γ. This is admittedly an oversimplification since the mixed-layer depth is not in equilibrium with the atmospheric forcing, but using a more refined model for m' and its relation with q' would not significantly alter our results. Under our assumption, the solution to (16) is

$$R_{Tq}(\tau) = \frac{n^2 + \gamma n}{1 + n^2 + 2n\gamma} \frac{C}{\nu} e^{\nu\tau},$$

$$\text{for } \tau \leq 0 \text{ (ocean leads)} \quad \text{and}$$

$$R_{Tq}(\tau) = \frac{n^2 + \gamma n}{1 + n^2 + 2n\gamma} \frac{C}{\nu} (2e^{-\lambda\tau} - e^{-\nu\tau}),$$

$$\text{for } \tau \geq 0 \text{ (ocean lags)}, \qquad (17)$$

where $C = \pi \nu F_{FF}(0)$ is the total stochastic forcing variance, and we have assumed $\nu \gg \lambda$. When T' leads, the
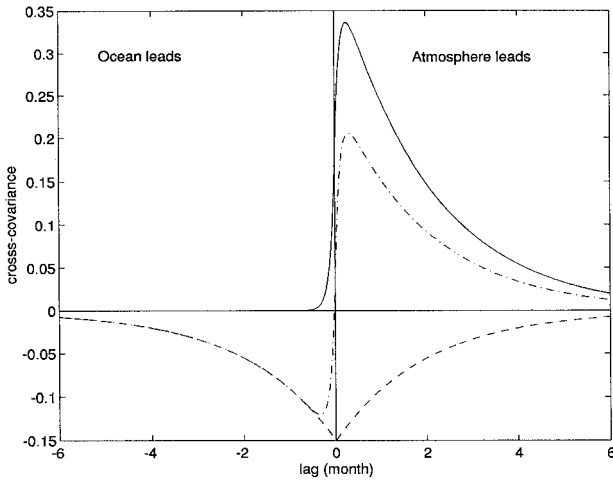
FIG. 1. Continuous line: Predicted covariance between T' and q' (in arbitrary units) as a function of time lag for $\nu = (3\ \text{day})^{-1}$, $n^2 = 2$, $\gamma = 0$, and $\lambda = (2\ \text{month})^{-1}$. Dashed line: Corresponding value of $-\lambda_a R_{TT}$ for $\lambda_a = (4\ \text{month})^{-1}$. Dashed–dotted line: Corresponding value of R_{TH}. The positive feedback case would be obtained by subtracting the first two curves instead of adding them.
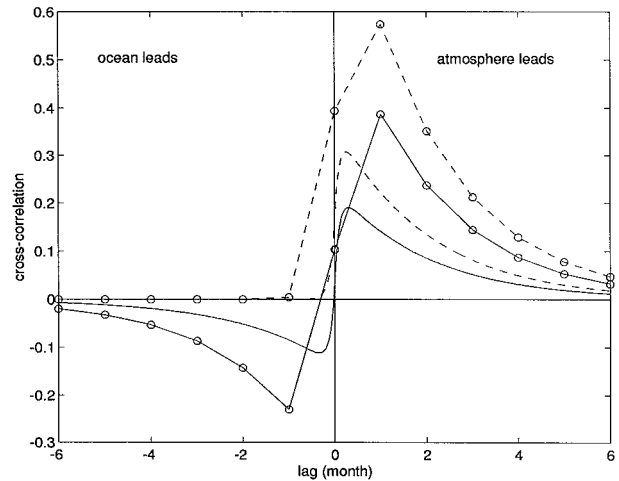

FIG. 2. Predicted correlation between T' and H' for no atmospheric feedback (dashed line) and for negative feedback (continuous line) when estimated from unaveraged (smooth curves) and monthly averaged (circle) data. Parameters are as in Fig. 1.

covariance R_{Tq} is negligible, except for lags of the order of the atmospheric persistence time. When T' lags, it has a positive maximum at small lag and then decreases slowly on the SST anomaly timescale. The smoothing associated with the use of monthly averages for the anomalies increases the cross correlation

$$r_{Tq}(\tau) = R_{Tq}(\tau)/[R_{TT}(0)R_{qq}(0)]^{1/2} \qquad (18)$$

by filtering out the high frequencies and shifts the maximum to lag zero or one, depending on the relative values of ν, λ, and T [see Eq. (A4) in the appendix and Fig. 2, dashed line]. This also holds for r_{Tm} and r_{TF}. Consequently, as first shown by Frankignoul and Hasselmann (1977), the correlation at zero lag between smoothed SST anomalies and atmospheric variables that are not (or only very little) affected by the SST anomalies (like sea level pressure or geopotential height) results from the atmospheric persistence and reflects the atmospheric forcing of the ocean, not the oceanic influence on the atmosphere. Empirical studies that interpret synchronous correlations or composites as indicative of the atmospheric response to SST anomalies (e.g., Palmer and Sun 1985; Peng et al. 1995) are thus misleading.

Since the heat flux term H' also contributes to the feedback, its covariance with T' differs from that of the stochastic forcing part. From (15), one finds

$$R_{TH}(\tau) = R_{Tq}(\tau) - \lambda_a R_{TT}(\tau), \qquad (19)$$

so the covariance between T' and H' is given by the difference between R_{Tq} and $\lambda_a R_{TT}$. Its shape and that of the corresponding correlation function r_{TH} critically depend on the sign of the atmospheric feedback (Frankignoul 1985; note that the meaning of terms H', q', λ_a, and λ_0 is not the same). For $\lambda_a > 0$ (negative feedback), $R_{TH}(\tau)$ and $r_{TH}(\tau)$ take an antisymmetric ap-

pearance, with negative values when T' leads, positive ones when it lags, and zero crossing near zero lag (Fig. 1). The deviation from pure antisymmetry and the magnitude of the correlation at positive and negative lags depends on the relative importance of the heat flux forcing, hence on n^2 and γ, and on λ_a. In particular, correlations for $\tau > 0$ (ocean lags) will dominate those for $\tau < 0$ (ocean leads) when n^2 is large (strong contribution of heat flux forcing) and λ_a small (weak atmospheric feedback). The correlation at zero lag depends on many parameters and can have either sign, hence it is more difficult to interpret. However, it will normally be positive when the primary role of the heat flux is the forcing one. As before, smoothing generally increases the correlation between T' and H' and shifts the maxima toward lags of plus and minus one, as illustrated in Fig. 2 (continuous line). For $\lambda_a < 0$ (positive feedback), the covariance is always positive and peaks for small positive lags (lag one when using smoothed values). Note from (19), (17), and (5) that is is only when the ocean leads that one part (the feedback part) of the two-way interaction can be singled out, and that in all cases the decay rate at large positive and negative lags is determined by the net feedback λ, not by the atmospheric one λ_a.

To estimate the atmospheric feedback λ_a from the observations, consider (17). For small lag, $R_{Tq}(\tau)$ critically depends on n^2, γ, ν, and λ_a, which are poorly known parameters, and it is thus of little help. However, for large negative lag ($\tau \ll -\nu^{-1}$), $R_{Tq}(\tau)$ is negligible and (19) yields

$$\lambda_a = -R_{TH}(\tau)/R_{TT}(\tau). \qquad (20)$$

When monthly anomaly data are available, the covariances at all lags less than or equal to -1 can be used in (20) to estimate λ_a, even though at large lags the data

are too noisy to provide useful information. Note that at lag -1 (20) neglects the small positive contribution of $R_{Tq}(-1)$, which is associated with atmospheric persistence [see (A4)], but the corresponding bias is very small. Relation (20) shows again that the information regarding predictability of the surface fluxes (hence the atmosphere) is contained in the correlation at negative lags when using monthly data, not in the simultaneous correlation.

The atmospheric feedback can also be derived from positive lags. Indeed, from (15) one can derive the following:

$$R_{HH}(\tau) = R_{qq}(\tau) - \lambda_a[R_{HT}(\tau) + R_{TH}(\tau)] - \lambda_a^2 R_{TT}. \quad (21)$$

For large positive lag, $R_{qq}(\tau)$ is negligible in (21), and the resulting quadratic equation in λ_a can be solved since the remaining terms can be estimated from the observations. However, this method is more sensitive to data noise and (20) is preferable.

Note that in regions where the mean current is large, the lag correlations should be considered nonlocally, and thus a more elaborate analysis is required. Complications also arise if the atmospheric forcing has a persistent component and is not white at low frequencies; estimates based on (20) would then be biased toward a too-weak negative feedback or a too-strong positive one. Since the atmospheric forcing in the North Pacific is influenced by persistent teleconnections from the equatorial Pacific, we will consider only observations in the central and eastern North Atlantic where the mean current is small and the tropical influence negligible.

In the following, the calculation is based on turbulent heat flux anomaly data, rather than on H', which depends on the mean mixed-layer depth. The turbulent heat flux feedback is thus obtained in W m^{-2} K^{-1} as in (1).

4. Turbulent heat flux feedback in the North Atlantic

Monthly fields of SST and sensible plus latent heat flux anomalies derived from the Comprehensive Ocean–Atmosphere Data Set were kindly provided on a $5° \times 5°$ grid by D. Cayan. The data have been described in Cayan (1992a). Here we consider the well-sampled 1952–92 period. Remaining data gaps were interpolated by successive linear interpolations. To decrease the influence of possible artificial trends in the reported winds, a third-order trend was removed at each grid point from both the SST and the heat flux anomaly data.

Since (4) applies only to midlatitude regions of weak mean surface current and eddy activity, we have excluded a broad western boundary current region and considered the central and eastern North Atlantic domain given in Fig. 4 below, where the mean surface current should be weaker than about 5 cm s^{-1} (Martel and Wunsch 1993). To reduce data and eddy noise, the
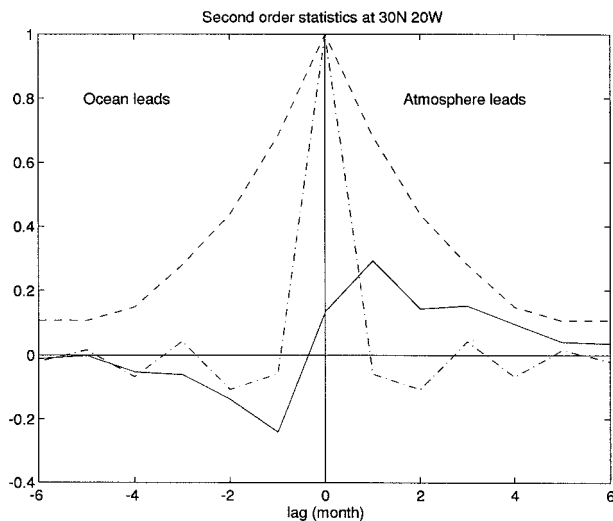

FIG. 3. Autocorrelation of observed SST (dashed line) and turbulent heat flux forcing (dashed–dotted line) anomalies at 20°W, 30°N, and cross correlation between the two variables (continuous line).

monthly SST and heat flux anomaly fields were filtered by performing an empirical orthogonal function (EOF) analysis and reconstructing the fields from the first 25 EOFs. For both variables, more than 95% of the original variance was retained.

a. Annual case

In agreement with (5), the SST anomaly autocorrelation function decays nearly exponentially at each grid point, as illustrated in Fig. 3 (dashed line). A small peak is often found near a lag of one year, reflecting the SST anomaly recurrence associated with mixed-layer deepening in late fall (Namias and Born 1970; Alexander and Deser 1995). The SST anomaly decay time was calculated by least squares fit over lags 0–3, using formula (A3) and assuming in addition that the SST data were contaminated by a small uncorrelated noise, which slightly improved the fit. As shown in Fig. 4, the decay time ranges between 1.5 months in the north and 4 months in the south. As the mean surface current is small but not negligible in the northern part of the domain, a slightly longer decay time would have been found by including SST anomaly advection in the stochastic model (Frankignoul and Reynolds 1983).

At each grid point of our North Atlantic domain, the cross-correlation function between SST and turbulent heat flux anomalies has an antisymmetric shape, which is in good agreement with our prediction for a negative heat flux feedback. As illustrated in Fig. 3 (continuous line), negative values are found when the ocean leads, peaking at lag -1, and often larger positive values occur when the ocean lags, with a maximum at lag 1 and an exponential decay thereafter. This statistical signature confirms that the turbulent heat flux anomalies contribute both to generating and damping the SST anomalies,
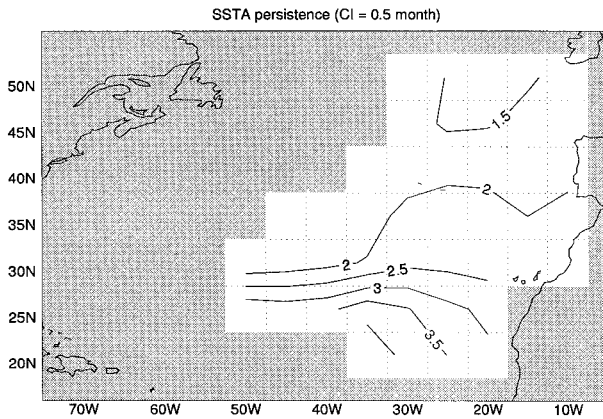
FIG. 4. SST anomaly decay time in months. The limits of the domain under study are indicated by the shading, and the grid boxes shown by the dotted lines.

FIG. 5. Estimated atmospheric heat flux feedback in W m^{-2} K^{-1}. Positive values indicate negative feedback.

and it suggests that the former effect generally dominates. However, other forcing and feedback play a role, as shown by the limited correlations and a frequent lack of pure antisymmetry. The dual role of the heat flux is also seen in the pattern analysis below and in the autocorrelation function of the turbulent heat flux anomalies (Fig. 3, dashed–dotted line), which becomes slightly negative for $|\tau| > 1$ month, as predicted by (21).

As discussed in section 3, the first few negative lags are best suited to estimate λ_a when using (20). We have chosen a weighted average of the lag -1, -2, and -3 estimates, using the exponential SST anomaly decay rates in Fig. 4 to define the weights:

$$\lambda_a = \frac{\lambda_a(-1) + e^{-\lambda}\lambda_a(-2) + e^{-2\lambda}\lambda_a(-3)}{1 + e^{-\lambda} + e^{-2\lambda}}, \quad (22)$$

where $\lambda_a(i)$ denotes the lag i estimates derived from (20). The results in Fig. 5 show that the negative turbulent heat flux feedback in the central and eastern North Atlantic has a mean value of about 20 W m^{-2} K^{-1}. The feedback depends on location, however, ranging between 10 and 15 W m^{-2} K^{-1} in the southern part of the domain and increasing toward the northwest and northeast where it reaches about 35 W m^{-2} K^{-1}. Maps based on a single negative lag or on lag 1 are basically similar but more noisy (not shown), although the lag -1 estimates are generally slightly lower, as expected from their small negative bias. In any case, the main features in Fig. 5 appear to be robust.

A comparison with (9)–(12) or with the feedback factor given in Han (1984) suggests that, on the spatial scale of the anomaly data, the surface air temperature adjustment to an SST anomaly should be about half the value of the latter, in agreement with recent adjustment estimates (Barsugli and Battisti 1998). In view of the observed SST anomaly persistence in Fig. 4, the damping effect of oceanic and atmospheric feedbacks should be roughly comparable. A more quantitative comparison
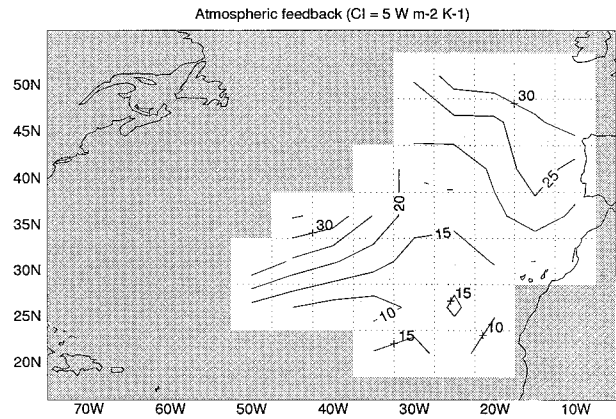
would require taking into account the large seasonal changes.

b. Scale-dependence and dominant interaction patterns

As recalled in section 1, it has been suggested that the negative atmospheric heat flux feedback should be weaker at larger scales. We tried to verify this by defining the SST and heat flux anomalies over increasingly larger regions before estimating the covariances, but in view of the strong geographical dependence of the feedback (Fig. 5), this could be done only by averaging the original data in regions with comparable values of λ_a. It was found that the stochastic forcing model applies equally well to larger geographical regions, but no significant dependence on the box size was found for λ_a, possibly because of the limited scale range that we could consider.

To emphasize the dominant patterns of variability, we have used two different methods. The first one is based on principal component analysis: the dominant modes of SST anomalies, the EOFs, have been calculated (no areal weighting) and the associated heat flux patterns at various lags obtained by regression onto the principal component time series. The second technique is the more powerful "maximum covariance analysis" based on a singular value decomposition (SVD) of SST and heat flux anomalies at different lags. As both give very similar results, we present only the EOF-based ones because the SST patterns remain fixed, while they vary slightly with lag in the SVD, which simplifies the interpretation.

Figures 6 and 7 (middle) show the first and second EOFs of the SST anomalies, which represents 37% and 17% of the variance. Although the EOF analysis was performed in our limited domain, the SST patterns were extended by regression to the western North Atlantic (shaded) to emphasize basin scales. Note that the extended EOF1 compares well to the second EOF of the

HFA regression on EOF1-SST (SST leads): CI = 2 W m-2

EOF1-SST of eastern and central Atlantic: CI = 0.1 K

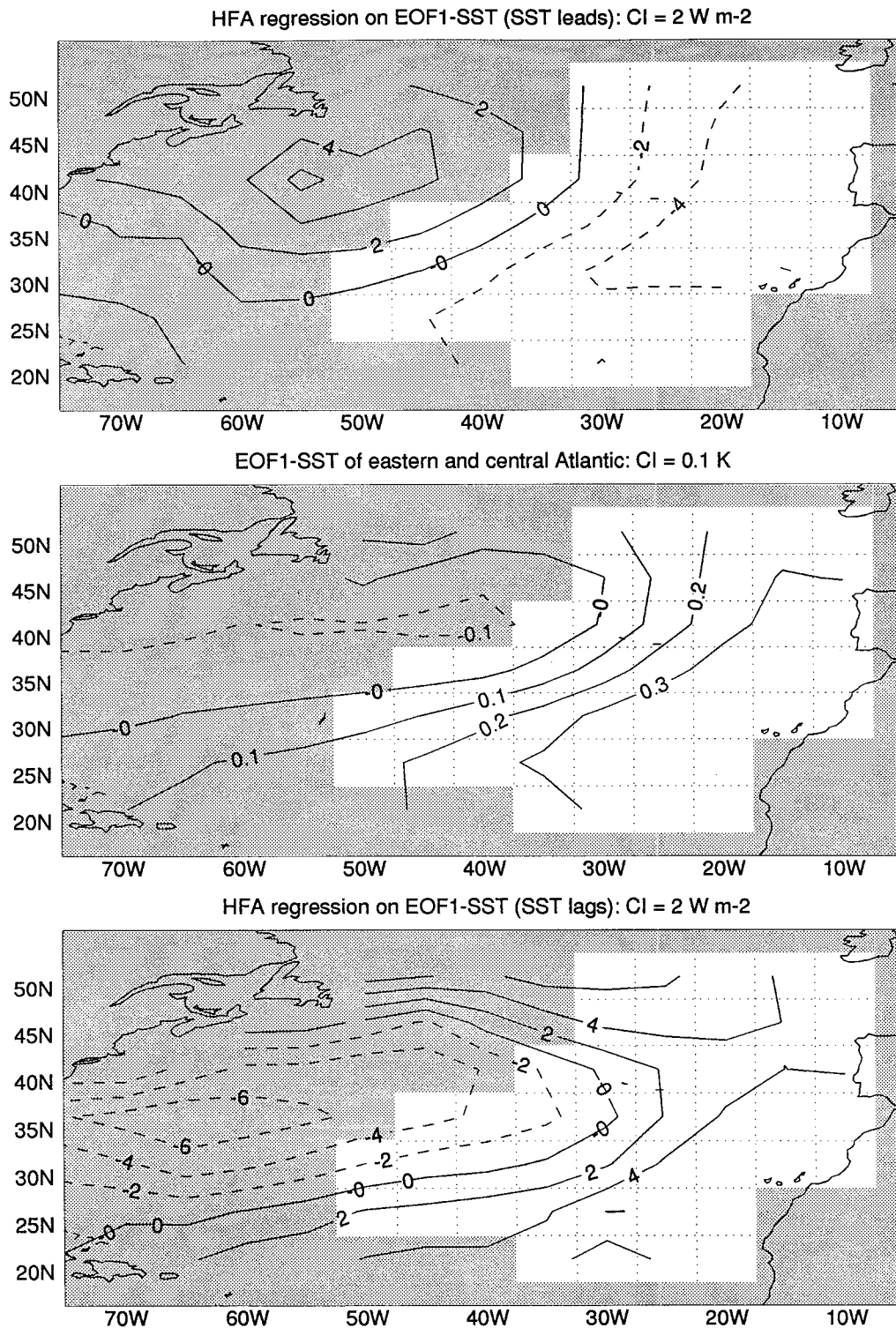## HFA regression on EOF1-SST (SST lags): CI = 2 W m-2

FIG. 6. (middle) First EOF of the SST anomalies in the central and eastern North Atlantic. The SST pattern has been extended to the western part of the basin by linear regression. The units are kelvins, and the principal component (not shown) is normalized. (top) Associated turbulent heat flux pattern one month later. (bottom) Associated turbulent heat flux pattern one month earlier, both in W m^{-2} K^{-1}.

HFA regression on EOF2-SST (SST leads): CI = 2 W m-2

EOF2-SST of eastern and central Atlantic: CI = 0.1 K

HFA regression on EOF2-SST (SST lags): CI = 2 W m-2
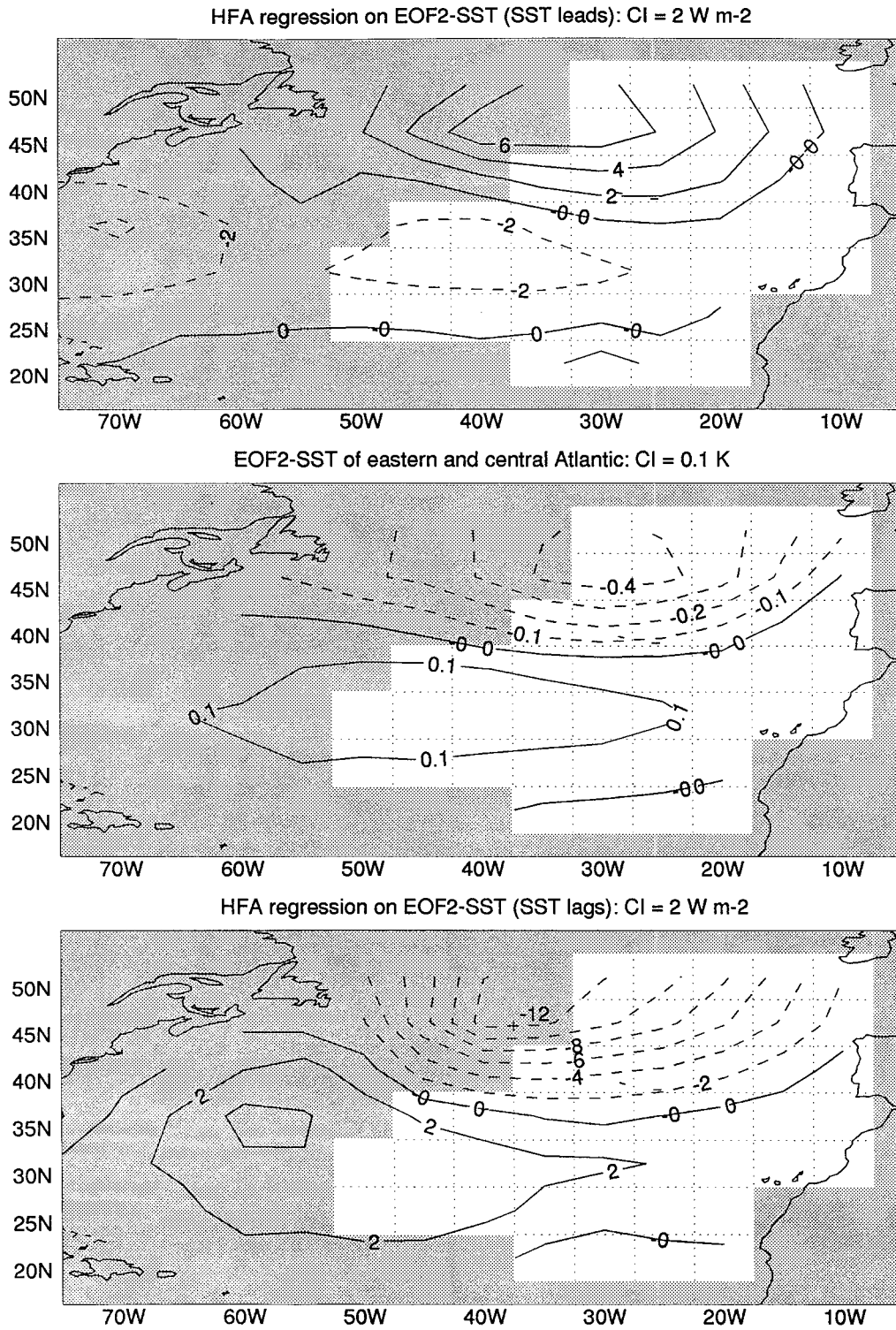
FIG. 7. As in Fig. 6 but for the second EOF.

SST anomalies in the whole domain (western North Atlantic included), while the extended EOF2 only loosely resembles the corresponding EOF1. Thus, somewhat different patterns were obtained by calculating the EOFs in whole domain, but the results below remained unchanged.

The heat flux patterns associated with the SST anomaly EOFs were obtained by regression onto the principal components using various lags. Again, this was done for the whole basin, but the patterns are only fully representative of the air–sea interactions in the limited domain. In Figs. 6 and 7, the heat flux anomalies are considered one month after and one month before the SST. The associated unlagged heat flux patterns (not shown) are mostly like those when the ocean lags, but with a weaker amplitude. When the ocean leads by one month, the associated heat flux patterns should primarily reflect the turbulent heat flux response to the SST anomaly modes. However, when the ocean lags, the interpretation is more complex since the heat flux pattern represents both the forcing of and the response to the SST anomaly mode [see (20) and Fig. 2]. As remarked earlier, it is only when the ocean leads that one part of the two-way interaction can be singled out.

When the ocean leads (Fig. 6, top), the heat flux pattern associated with the SST EOF1 is nearly in phase with the latter in the limited domain, and its sign indicates that it damps the SST anomaly. The negative feedback is thus primarily local, although the heat flux might be shifted a half-grid box to the south and the west of the SST (a similar shift appears in the SVD). This westward shift is smaller than predicted by the simple linear wave theory of Frankignoul (1985), as can also be inferred from the numerical experiment of Bladé (1997). Accordingly, the eastward propagator effect of the atmospheric feedback should be small. In the western North Atlantic (shaded), the SST and heat flux patterns remain similar, although less strikingly. Note, however, that a little distortion of the SST pattern by the larger currents is expected during the 1-month lag. In any case, the feedback seems to remain negative, in fact more so than farther to the east, and this was also found with the full domain EOFs. When the ocean lags (Fig. 6, bottom), the associated heat flux pattern has the opposite sign, consistent with the atmosphere forcing the ocean, and again remarkably resembles that of the SST, except that it is shifted south by about one grid size.

Similar results are found for the regression of the turbulent heat flux onto the second SST anomaly principal component (Fig. 7). When the ocean leads (top), the heat flux in the limited domain is nearly exactly out of phase with the SST anomaly (negative feedback), and when it lags, it is nearly exactly in phase. Again, the heat flux feedback seems to be mostly negative in the western North Atlantic (shaded), but the SST patterns is a dipole in the north–south direction, so that a small shift in the east–west direction would be hard to detect.

The spatial coincidence between the SST and heat flux modes in the case where the ocean lags was noted by Cayan (1992a), who compared the rate of change of wintertime SST anomalies to the turbulent heat flux anomalies. However, the remarkable similarity in the associated heat flux patterns at lag −1 and 1, but for a change of sign, does not seem to have been noted before. This similarity in lead and lag situations may result from (7) and (8). As discussed by Cayan (1992b) and Battisti et al. (1995), the surface air temperature and humidity changes are fundamental to the turbulent heat flux anomalies and tend to play a larger role in the extratropics than the changes in the wind magnitude. As they are largely forced by the surface heat exchanges, the patterns of the dominant SST anomalies at any given time will resemble those of the air temperature during the preceding period, which reflects the dominant modes of atmospheric variability. Now consider the persistent SST signal in (7) and (8). If an SST anomaly had no effect on air temperature and humidity, the fluctuations in the latter would be uncorrelated with the SST on the SST anomaly timescale, in view of the stochastic nature of the short timescale atmospheric variability. Thus, a persistent anomaly with the opposite sign but the same pattern as the SST anomaly would appear in the surface heat flux. As a result, the associated heat flux patterns should be similar but of opposite sign at lead and lag relations. This should hold if the atmospheric boundary layer adjusts somewhat to the SST changes.

5. Seasonal variations of the heat flux feedback

The persistence of the SST anomalies depends on the season, reflecting not only the changes in the mixed-layer depth but also in the feedback processes, for instance, in the entrainment feedback, which is strongest during fall when the mixed layer is deepening (Frankignoul 1985). The atmospheric response to SST anomalies is also strongly dependent on season, and correspondingly large seasonal changes in the heat flux feedback have been found in AGCM experiments (e.g., Peng et al. 1995).

We have first estimated the turbulent heat flux feedback by only considering winter or summer months. The calculation is less accurate than with the full dataset as there are fewer degrees of freedom in the covariance estimates, and also because the variance of each field in (20) has strong but different seasonal variations. Indeed, the variance of the SST anomalies is at maximum in early summer and minimum in late winter, while that of the heat flux anomalies peaks in early winter and is at minimum during summer. To reduce the impact of these variations, we have estimated λ_a, from the lag −1 covariances only, instead of using (22), which further increases the estimation noise. Winter is defined from December through March for the heat flux and from November through February for SST, and summer from
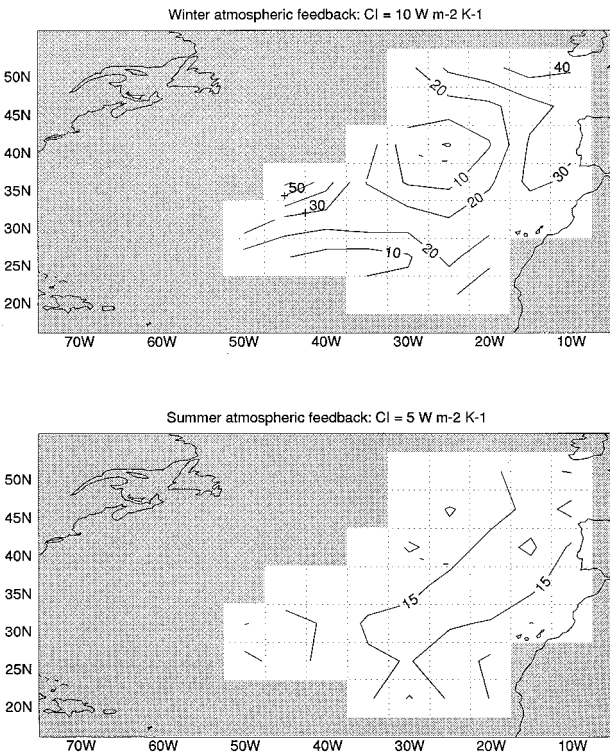
FIG. 8. Estimated atmospheric heat flux feedback in W m^{-2} K^{-1} in winter (top) and summer (bottom). Positive values indicate negative feedback.

FIG. 9. SST anomaly decay time in month during winter (top) and summer (bottom).

June through September for the heat flux and from May through August for SST.

As shown in Fig. 8 (top), the negative heat flux feedback is strong in winter and its pattern resembles the yearly one. Although the estimates are more noisy and the precise values should be viewed with caution, the feedback seems particularly strong in the northwestern corner and in the north, and there is a marked minimum in a broad region around 25°W, 40°N. In contrast, during summer (bottom) the feedback is weak and more uniform, averaging 10–15 W m^{-2} K^{-1} and decreasing toward the southwest. For comparison we show in Fig. 9 an estimate of the corresponding SST anomaly decay time, which is only a little larger in winter than in summer, even though the mixed-layer depth is much larger. This suggests that the SST persistence critically depends on the strength of the oceanic and the atmospheric feedbacks. Note the enhanced persistence of the wintertime SST anomalies around 25°W, 40°N where the atmospheric feedback is minimum.

To describe more completely the seasonal variations of the heat flux feedback, we have constructed its averaged seasonal cycle in several 15° × 15° boxes, using three (instead of four) consecutive months to estimate the covariances for finer temporal resolution. The feedback is estimated by the average of the nine estimates in each box (since they contain nine grid points), and the accuracy of the estimates can be assessed from their
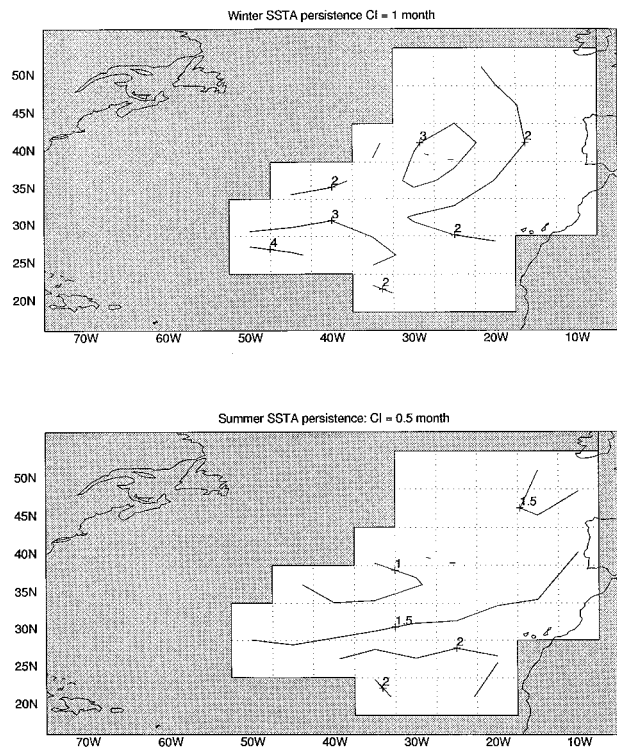
standard deviation. Note that the estimates for consecutive months are not independent as the data are overlapping in time. As illustrated in Fig. 10 (top), the negative feedback in the eastern Atlantic has a large seasonal cycle at high latitudes. It is strongest in early fall when it reaches more than 40 W m^{-2} K^{-1} but decreases rapidly to a minimum of less than 10 W m^{-2} K^{-1} in midwinter; it then varies between about 10 and 20 W m^{-2} K^{-1} until early summer, when it starts increasing rapidly. In the subtropics (Fig. 10, bottom), the seasonal cycle is less marked, and λ_a stays near 15 W m^{-2} K^{-1}, except for a minimum of about half this value in late winter. Overall, the largest negative turbulent heat flux feedback is usually reached in early fall and the smallest one in late winter. However, in the western part of the domain near 35°N, the largest negative feedback is reached in December–January. This can be seen by comparing Fig. 8 (top) to Fig. 11.

In their AGCM experiments, Peng et al. (1995) found a strong positive heat flux feedback in November conditions and an even stronger negative one in January conditions. Although the (positive) SST anomaly was centered around 45°W, 47°N, hence mostly to the northwest of our limited domain, we have mapped for comparison λ_a for a 3-month period centered around October for SST and 1 month later for the turbulent heat flux (Fig. 11). The observations indicate that the turbulent heat flux feedback is always negative, at least in the central and eastern North Atlantic.
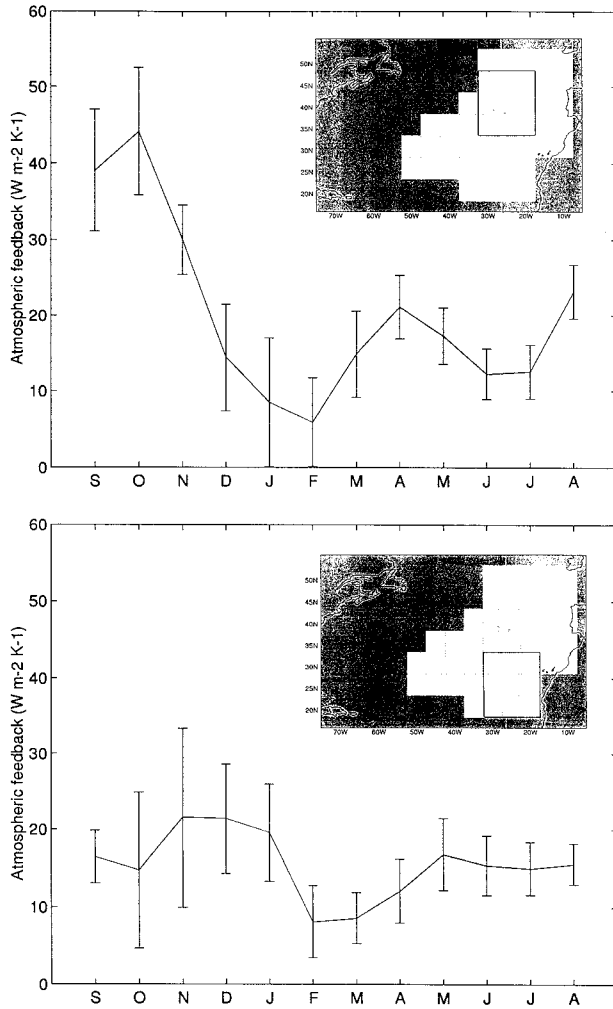
FIG. 11. Estimated atmospheric heat flux feedback in W m^{-2} K^{-1} in early fall, based on OND for the heat flux and SON for SST. Positive values indicate negative feedback.

FIG. 10. Seasonal cycle of the atmospheric feedback in W m^{-2} K^{-1} in $15° \times 15°$ boxes centered on 25°W, 40°N (top) and 25°W, 25°N (bottom). Estimates are based on overlapping 3-month intervals centered for SST on the month indicated in abscissa. The error bar indicates one standard deviation for each estimate.

6. Surface boundary conditions and the SST–evaporation feedback

Our analysis confirms that, to a first approximation, the turbulent heat flux acts as a linear damping on the monthly SST anomalies, although with a weaker coupling coefficient than usually assumed in ocean-only simulations. Lacking sufficiently accurate cloud data, we have not attempted to investigate the feedback effects of the radiation fluxes. Some studies show that the changes in marine stratus cloud coverage are negatively correlated with the SST and may thus contribute a small positive feedback, especially during summer (e.g., Norris and Levoy 1994), but causes and effects are again difficult to distinguish. In atmospheric models, the feedback due to the radiation flux can be negative (Power et al. 1995) or positive (Seager et al. 1995), but its
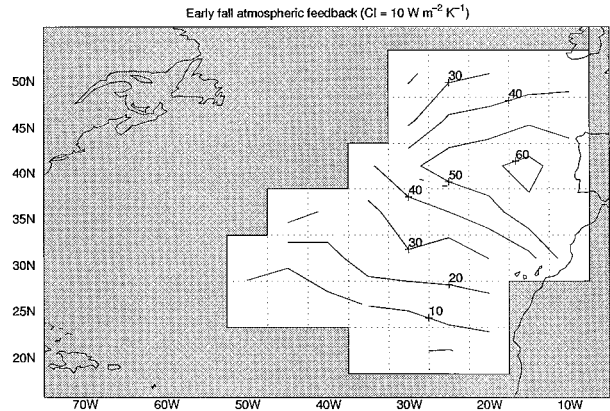
contribution in both cases is very small, probably below the noise level of our calculation.

Except north of 40°N, the turbulent heat flux is dominated by the flux of latent heat (Cayan 1992b), and it is mainly the evaporation that acts as a restoring factor. Thus, as noted by Hughes and Weaver (1996), the traditional mixed boundary conditions should be modified to include the "SST–evaporation feedback" and allow SST changes to indirectly affect the sea surface salinity (SSS). To investigate how this feedback links SSS and SST anomalies, we add salinity to the slab mixed-layer model. Following the steps used to derive (3), the SSS anomaly equation is approximately given by

$$\frac{dS'}{dt} \approx -\frac{\mathbf{u}'_E \cdot \overline{\nabla S}}{\overline{h}} - \frac{h'}{\overline{h}}\partial_t \overline{S} - \frac{[\Gamma(w_e)w_e(S - S^-)]'}{\overline{h}} + \frac{\overline{S}(E' - P')}{\overline{h}} + \kappa\nabla^2 S', \quad (23)$$

where S denotes SSS, E evaporation, and P precipitation (both per unit specific mass). Using (15), the evaporation anomaly can be written in our formalism as

$$E' = e' + \frac{\lambda_a C_p \overline{h}}{L(1 + B)}T', \quad (24)$$

where e' represents the stochastic part of the evaporation changes and B is the Bowen ratio between sensible and latent heat flux. The relation between evaporation and precipitation anomalies in the midlatitudes is unlikely to be local for small SST anomalies [see discussion in Hughes and Weaver (1996)], hence we simply assume that the SST-induced evaporation changes are not balanced by a corresponding change in precipitation. The effect of the SST–evaporation feedback on the SSS rate of change is then represented in (22) by $\lambda_e T'$, with

$$\lambda_e = \frac{\lambda_a C_p \overline{S}}{L(1 + B)}. \quad (25)$$

Using as typical midlatitude values $\overline{S} = 36.5$ psu, $B =$

0.2, and $\rho C_p \overline{h} \lambda_e = 20$ W m^{-2} K^{-1} yields $\lambda_e \approx 3.5 \times 10^{-9}$ psu s^{-1} K^{-1} for $\overline{h} = 70$ m. In two months, a sustained SST anomaly of 1 K would create only an SSS anomaly of about 0.02 psu, so the effect is small at the interannual timescale. However, as the SSS anomaly is linear in t, long-lasting SST anomalies should have more impact, and the SST–evaporation feedback may contribute substantially to the SSS variations at decadal and longer timescales. Hughes and Weaver (1996) have investigated some of its effects on the thermohaline circulation.

7. Conclusions

In the central and eastern Atlantic where the mean surface current is small, the extratropical SST anomalies are well simulated by a one-dimensional mixed-layer model that is stochastically forced by the atmosphere. Using the lag covariance between surface heat flux and SST anomalies, we have shown that the turbulent heat flux plays a dual forcing and damping role, and we have estimated the local turbulent heat flux feedback from the observations. The feedback is negative and averages around 20 W m^{-2} K^{-1}, and it varies with location and season, being larger in the fall and smaller in summer. There is no evidence that the feedback can become significantly positive. These estimates are in broad agreement with the response of most AGCMs to prescribed SST anomalies, but they do not support the results of Peng et al. (1995), who found that in November conditions the heat flux feedback would be strongly positive. Their SST anomaly was mostly to the northwest of our limited domain, and different atmospheric dynamics may be at play when the SST forcing is closer to the storm track. Yet the main patterns of air–sea interaction suggest that the feedback remains negative in the western Atlantic, although its estimation was not attempted here since nonlocal effects due to SST anomaly advection are important in this region. Note also that the heat flux feedback was speculated to be positive between 50° and 60°N by Grötzner et al. (1998) in the ECHO coupled GCM. Although this region lies mostly to the north of our domain, this hypothesis is not consistent with our analysis where the trend is toward a northward increase in negative feedback. Thus, surface heat exchanges are unlikely to contribute to sustaining decadal oscillations in the North Atlantic.

It is not known whether the turbulent heat flux feedback is also negative in the North Pacific, or whether it can become strongly positive as in the GCM experiment of Latif and Barnett (1994), thereby contributing to the existence of an interdecadal North Pacific coupled mode. This will be more difficult to establish from observations because the feedback factor can be estimated only by the present method if the heat flux is represented to a good approximation by a white noise forcing plus a local SST effect. This is not the case in the North Pacific where there is in addition a persistent ENSO influence, but the latter can perhaps be removed.

Finally, this analysis provides some support for the use of an SST restoring term in ocean-only simulations, with a magnitude that is in reasonable agreement with the estimates of Seager et al. (1995) and Power et al. (1995), but it applies only to short timescale SST variability. On timescales much longer than seasonal, the air temperature (or the restoring temperature) should be allowed to vary and nonlocal influences considered, and there is no substitute for a proper representation of the atmospheric dynamics. Nonetheless, if mixed boundary conditions are used in ocean-only simulations, the SST–evaporation feedback needs to be included since the turbulent heat flux feedback is primarily due to the flux of latent heat, and the associated evaporation should significantly affect the SSS variability on decadal and longer timescales.

APPENDIX

Smoothing Effects on the Covariance Functions

As pointed out by Frankignoul and Hasselmann (1977), the smoothing due to the use of monthly averages in anomaly data must be taken into account in the comparison between modeled and observed lag correlations and covariances. If we denote by $Z(t)$ the monthly average of a variable, z,

$$Z(t) = \frac{1}{T} \int_{-T/2}^{T/2} z(t - t') \, dt', \qquad (A1)$$

where T is one month, its autocovariance is given by

$$R_{ZZ}(\tau) = \left\langle \frac{1}{T} \int_{-T/2}^{T/2} z(t + \tau - t') \, dt' \frac{1}{T} \int_{-T/2}^{T/2} z(t - t'') \, dt'' \right\rangle$$

$$= \frac{1}{T^2} \int_{-T/2}^{T/2} dt' \int_{-T/2}^{T/2} dt'' \, R_{ZZ}(\tau - t' + t''). \quad (A2)$$

Thus, the autocovariance of the SST anomaly, given to a good approximation by (5), becomes

$$R_{TT}(\tau) = \frac{\pi}{\lambda} F_{FF}(0) \left(\frac{2}{\lambda T} \right)^2 sh^2 \frac{\lambda T}{2} e^{-\lambda \tau}, \quad \text{for } |\tau| \geq 1,$$

$$= \frac{\pi}{\lambda} F_{FF}(0) \frac{2}{(\lambda T)^2} [\lambda T + e^{-\lambda T} - 1], \quad \text{for } \tau = 0,$$

$$(A3)$$

so it decays only exponentially for $\tau > 1$.

In the same way, the covariance between monthly averages of T' and q' is found to be, from (17),

$$R_{Tq}(\tau) = \pi F_{FF}(0)\frac{n^2 + \gamma n}{1 + n^2 + 2\gamma n}\left(\frac{2}{\nu T}\right)^2 sh^2\left(\frac{\nu T}{2}\right)e^{\nu \tau},$$

$$\text{for } \tau < 0$$

$$= \pi F_{FF}(0)\frac{n^2 + \gamma n}{1 + n^2 + 2\gamma n}\frac{2}{(\lambda T)^2}(\lambda T + e^{-\lambda T} - 1),$$

$$\text{for } \tau = 0, \quad \text{and}$$

$$= \pi F_{FF}(0)\frac{n^2 + \gamma n}{1 + n^2 + 2\gamma n}$$

$$\times \left[2\left(\frac{2}{\lambda T}\right)^2 sh^2\left(\frac{\lambda T}{2}\right)e^{-\lambda \tau} - \left(\frac{2}{\nu T}\right)^2 sh^2\left(\frac{\nu T}{2}\right)e^{-\nu \tau}\right],$$

$$\text{for } \tau > 0. \tag{A4}$$

The covariance between monthly SST and heat flux anomalies is readily obtained from (A3) and (A4), using (19).

REFERENCES

Alexander, M. A., and C. Deser, 1995: A mechanism for the recurrence of wintertime midlatitude SST anomalies. *J. Phys. Oceanogr., 25,* 122–137.

——, and C. Penland, 1996: Variability in a mixed layer ocean model driven by stochastic atmospheric forcing. *J. Climate, 9,* 2424–2442.

Barsugli, J. J., and D. S. Battisti, 1998: The basic effects of atmosphere–ocean thermal coupling on midlatitude variability. *J. Atmos. Sci., 55,* 477–493.

Battisti, D. S., U. Bhatt, and M. A. Alexander, 1995: A modeling study of the interannual variability in the wintertime North Atlantic Ocean. *J. Climate, 8,* 3067–3083.

Bladé, I., 1997: The influence of midlatitude ocean/atmosphere coupling on the low-frequency variability of a GCM. Part I: No tropical SST forcing. *J. Climate, 10,* 2087–2106.

Bretherton, F. P., 1982: Ocean climate modeling. *Progress in Oceanography,* Vol. 11, Pergamon, 93–129.

Bryan, F., 1986: High-latitude salinity effects and interhemispheric thermohaline circulations. *Nature, 323,* 301–304.

Cayan, D. R., 1992a: Latent and sensible heat flux anomalies over the northern oceans: Driving the sea surface temperature. *J. Phys. Oceanogr., 22,* 859–881.

——, 1992b: Latent and sensible heat flux anomalies over the northern oceans: The connection to monthly atmospheric circulation. *J. Climate, 5,* 334–369.

Chen, F., and M. Ghil, 1995: Interdecadal variability of the thermohaline circulation and high-latitude surface fluxes. *J. Phys. Oceanogr., 25,* 2547–2568.

Frankignoul, C., 1985: Sea surface temperature anomalies, planetary waves and air–sea feedback in the middle latitudes. *Rev. Geophys., 23,* 357–390.

——, 1995: Climate spectra and stochastic climate models. *Analysis of Climate Variability. Application of Statistical Techniques,* H. Von Storch and A. Navarra, Eds., Springer–Verlag, 29–50.

——, and K. Hasselmann, 1977: Stochastic climate models. Part II: Application to sea-surface temperature variability and thermocline variability. *Tellus, 29,* 284–305.

——, and R. W. Reynolds, 1983: Testing a dynamical model for

midlatitude sea surface temperature anomalies. *J. Phys. Oceanogr., 13,* 1131–1145.

Grötzner, A., M. Latif, and T. P. Barnett, 1998: A decadal climate cycle in the North Atlantic Ocean as simulated by the ECHO coupled GCM. *J. Climate, 11,* 831–847.

Han, Y.-J., 1984: A numerical World Ocean general circulation model. Part II: A baroclinic experiment. *Dyn. Atmos. Oceans, 8,* 141–172.

Haney, R. L., 1971: Surface thermal boundary condition for ocean circulation models. *J. Phys. Oceanogr., 1,* 241–248.

Herterich, K., and K. Hasselmann, 1987: Extraction of mixed layer advection velocities, diffusion coefficients, feedback factors and atmospheric forcing parameters from the statistical analysis of North Pacific SST anomaly fields. *J. Phys. Oceanogr., 17,* 2145–2156.

Hughes, T. M. C., and A. J. Weaver, 1996: Sea surface temperature–evaporation feedback and the ocean's thermohaline circulation. *J. Phys. Oceanogr., 26,* 644–654.

Kleeman, R., and S. Power, 1995: A simple atmospheric model of surface heat flux for use in ocean modeling studies. *J. Phys. Oceanogr., 25,* 92–105.

Kushnir, Y., and N.-C. Lau, 1992: The general circulation model response to a North Pacific SST anomaly: Dependence on time scale and pattern polarity. *J. Climate, 5,* 271–283.

——, and I. M. Held, 1996: Equilibrium atmospheric response to North Atlantic SST anomalies. *J. Climate, 9,* 1208–1220.

Latif, M., and T. P. Barnett, 1994: Causes of decadal climate variability in the North Pacific/North American sector. *Science, 266,* 634–637.

Marotzke, J., and J. Willebrand, 1991: Multiple equilibria of the global thermohaline circulation. *J. Phys. Oceanogr., 21,* 1372–1385.

Martel, F., and C. Wunsch, 1993: The North Atlantic circulation in the early 1980s—An estimate from inversion of a finite difference model. *J. Phys. Oceanogr., 23,* 898–924.

Molchanov, S. A., O. I. Piterbarg, and D. D. Sokolov, 1987: Generation of large-scale ocean temperature anomalies by short-period atmospheric processes. *Izv. Atmos. Ocean Phys., 23,* 405–409.

Namias, J., and R. M. Born, 1970: Temporal coherence in North Pacific sea surface temperature patterns. *J. Geophys. Res., 75,* 5952–5955.

Norris, J. R., and C. B. Leovy, 1994: Interannual variability in stratiform cloudiness and sea surface temperature. *J. Climate, 7,* 1915–1925.

Palmer, T. M., and Z. Sun, 1985: A modelling and observational study of the relationship between sea surface temperature in the northwest Atlantic and the atmospheric general circulation. *Quart. J. Roy. Meteor. Soc., 111,* 947–975.

Peng, S., L. A. Mysak, H. Richtie, J. Derome, and B. Dugas, 1995: The differences between early and midwinter atmospheric responses to sea surface temperature anomalies in the northwest Atlantic. *J. Climate, 8,* 137–157.

Power, S. B., R. Kleeman, R. A. Colman, and B. J. McAvaney, 1995: Modeling the surface heat flux response to long-lived SST anomalies in the North Atlantic. *J. Climate, 8,* 2161–2180.

Rahmstorf, S., and J. Willebrand, 1995: The role of temperature feedback in stabilizing the thermohaline circulation. *J. Phys. Oceanogr., 25,* 787–805.

Reynolds, R. W., 1978: Sea surface temperature anomalies in the North Pacific Ocean. *Tellus, 30,* 97–103.

Seager, R., Y. Kushnir, and M. A. Cane, 1995: On heat flux boundary conditions for ocean models. *J. Phys. Oceanogr., 25,* 3219–3230.

Stommel, H., 1961: Thermohaline convection with two stable regimes of flow. *Tellus, 13,* 224–230.

Weaver, A. J., and E. S. Sarachik, 1991: Evidence for decadal variability in an ocean general circulation model: An advective mechanism. *Atmos.–Ocean, 29,* 39–60.

Yin, F. L., and E. S. Sarachik, 1995: Interdecadal thermohaline oscillations in a sector ocean general circulation model: Advective and convective processes. *J. Phys. Oceanogr.,* **25,** 2465–2484.

Zhang, S., R. J. Greatbatch, and C. A. Lin, 1993: A reexamination of the polar halocline catastrophe and implications for coupled ocean–atmosphere modeling. *J. Phys. Oceanogr.,* **23,** 287–299.